

Abstract—Can you move along a surface in space without propellant or physical contact? On-orbit servicing requires a robot to operate in close proximity to the surface of a target spacecraft in order to inspect, refuel, or repair it. Robotic operation in close proximity is difficult in space because spacecraft are fragile and often have poorly known, undamped dynamics. Current actuators for locomotion and grasping during on-orbit servicing require physical contact with the target (dangerous), propellant (expensive), or cooperation from the target (often infeasible.) This paper presents a new actuator - the induction coupler - that generates eddy-current forces between a robotic orbital inspector and the conductive exterior of its target. These forces allow the inspector to crawl along the surface of a target *without physical contact*. Sets of induction couplers composed of spinning arrays of permanent magnets can exert control forces and torques in all six rigid-body degrees of freedom by strategically repelling and shearing across the surface of the target. This paper uses an analytical model of eddy-current forces to simulate the set of manoeuvres necessary to generate the control forces and torques that can move and orient a robotic orbital inspector. Experiments on a low-friction test bed demonstrate a successful implementation of the actuator and verify the manoeuvres.

I. INTRODUCTION

On-orbit servicing (OOS) is a valuable but difficult robotic task. [2][3][4] Just as on earth, large assets like the International Space Station (ISS) or geostationary satellites experience wear and unexpected problems that require inspection, repair, or refuelling.[5] [10] These tasks are well suited for robots because it is less dangerous and expensive to send an inspection vehicle to geostationary orbit or outside the ISS than a human spacewalker.

Manoeuvring close to a target is essential to OOS and is a particularly risky proposition on orbit. There are presently three methods for an inspector to manoeuvre close to the surface of its target: it can physically grapple the surface to pull itself along; it can use propellant and thrusters; or it can use cooperative, non-contacting electromagnetic systems installed both on the inspector and the target. Grappling has many potential risks in an uncertain, low-friction environment. Propellant is expensive and can damage sensitive targets. Cooperation is infeasible in many situations because most spacecraft launch without the necessary subsystems: spacecraft are *not* designed to be inspected or repaired by robots.

However, the ISS and most spacecraft are composed of aluminium plates, curves, and beams. By introducing a changing magnetic field, a robotic inspector can induce eddy currents in these non-magnetic but conductive components and use the reaction force between the field and the currents for actuation.[11] These eddy-current forces have several

terrestrial applications from trash separation [9] to maglev propulsion,[8][6] but have never been used in either robotics or orbital context. An eddy-current based actuator called an induction coupler, can provide a completely new way to perform robotic locomotion and manipulation in space.

The first step towards an induction coupler locomotion system is to show how to produce actuation in each degree of freedom (DoF). What is it capable of going through different states? Eddy-current forces depend both on the robot's pose and the geometry of the environment. Simulating general eddy-current forces is normally done with finite element analyses (FEA) [1]. FEA are unsuitable for dynamically modelling induction couplers for two reasons: they are both too slow to run at each time step and their mesh of nodes needs change with the geometry of the system. Paudel and Bird derived an extensible analytical solution for eddy-current forces near a flat plate that enables fast simulations of induction couplers.[7]

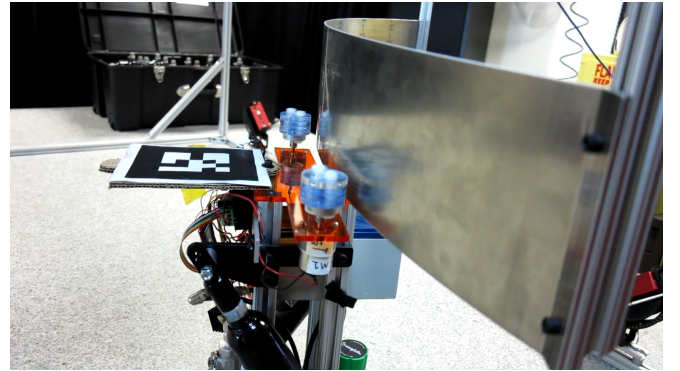


Fig. 1. An experimental induction coupled inspector moving near a model of the ISS exterior.

Section II presents an analytical model to solve for induction coupler forces. Section III describes and simulates the necessary open-loop manoeuvres to move in each dof. Finally, Section V presents experimental verification of each manoeuvre with a prototype induction coupler system on a low-friction testbed, shown in figure 1.

II. ACTUATOR MODEL

Paudel and Bird derived an analytical solution for the force from a single rotating array of permanent magnets near a flat conductor. [7] In a reference frame attached to the conductive surface shown in figure 2, the force on the magnet array is

$${}^S\mathbf{F} = \frac{w}{8\pi\mu_0} \int_{-\infty}^{\infty} \Gamma(\xi, g) |B^s(\xi, g)|^2 d\xi \quad (1)$$

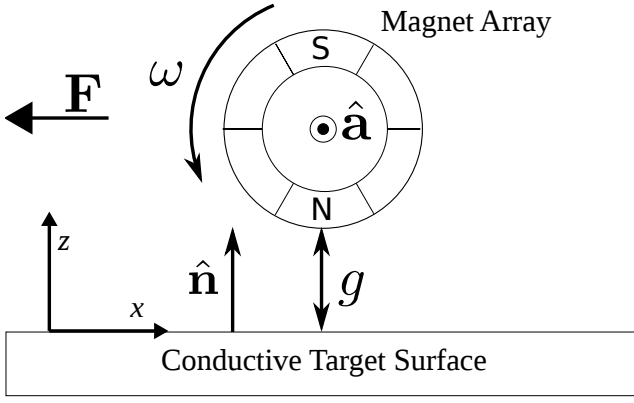


Fig. 2. Diagram of a single induction coupler array

Here Γ is a transmission function associated with the inductive surface and B is the non-time-varying part of the array's magnetic field Fourier transformed with respect to \hat{x} . Γ and B are nonlinear functions of the system state. Γ depends on the array's rotation frequency ω , velocity \mathbf{v} and distance from the surface. B is a nonlinear function of g as well. Near a curved surface, the assumption of an infinite flat surface is *locally* valid for induction couplers because the operating gap is on the order of centimeters: very small compared to the curvatures of most target surfaces.

A geometric generalization of this force is informative in order to dynamically model the actuation of a 6-DoF orbital inspector. Eddy-current forces act only in opposition to change in magnetic field, so the net force will always act perpendicular to the array's spin axis. Thus, a 3D formulation of the force in any reference frame can be found by tilting the force plane (shown in figure 2 along with $\hat{\mathbf{n}}$).

$$\mathbf{F} = F_z(g, \omega, \mathbf{v}) (\hat{\mathbf{a}} \times \hat{\mathbf{n}}) + F_y(g, \omega, \mathbf{v}) (\hat{\mathbf{a}} \times \hat{\mathbf{n}}) \times \hat{\mathbf{a}} \quad (2)$$

F_z and F_y are the components of the planar force calculated in equation 1. This statement of eddy-current forces is powerful because it is both analytical and general. The generality enables fast simulations of a 6-DoF inspection vehicle while the analytical nature will enable provable statements about the systems stability. A full system consists of several arrays to control all six degrees of freedom. The net force and torque on the body then depends on the location and orientation of n arrays in the inspector's frame. Each array rotates around an axis, $\hat{\mathbf{a}}_n$, located at \mathbf{d}_n , shown in figure 3. The net control force is

$$\mathbf{F}_{net} = \sum_i F_z (\hat{\mathbf{a}}_i \times \hat{\mathbf{n}}_i) + F_y (\hat{\mathbf{a}}_i \times \hat{\mathbf{n}}_i) \times \hat{\mathbf{a}}_i \quad (3)$$

and the net control torque is

$$\boldsymbol{\tau}_{net} = \sum_i \mathbf{d}_i \times [F_z (\hat{\mathbf{a}}_i \times \hat{\mathbf{n}}_i) + F_y (\hat{\mathbf{a}}_i \times \hat{\mathbf{n}}_i) \times \hat{\mathbf{a}}_i] \quad (4)$$

\mathbf{n}_i is the vector to the surface segment closest to array i .

The following sections use this model to demonstrate how a robotic inspector can use induction couplers to generate forces and torques in all six rigid body degrees of freedom.

III. MOVEMENT PRIMITIVES

A. Planar Movement

While moving in the plane parallel to the target surface, induction couplers act similar to contactless wheels - they generate forces parallel to the surface that increase with their speed. Thus, a fixed arrangement needs at least two couplers to move in all three planar degrees of freedom and three couplers to control each degree of freedom independently. Unlike wheels, induction couplers do not provide constraint forces perpendicular to their rotation. They also cannot slip on the surface. So unlike wheels that skid if they accelerate too quickly, induction coupler forces are limited only by the capabilities of their motors.

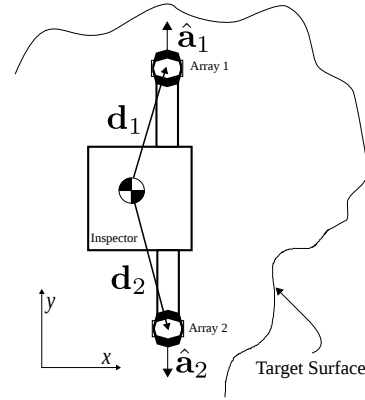


Fig. 3. Configuration for planar control

An inspector can translate in the plane by using a pair of induction couplers like differential drive wheels. Figure 3 shows this mode. Ideally, pure translational motion will involve no net torque. Because there are no kinetic constraints on the couplers the net torque they generate is extremely sensitive to their relative location to the system's center of mass (CoM). This sensitivity means that in open loop operation any unaccounted asymmetry between the two induction couplers will lead to unwanted torque. Thus, any induction coupler system will need closed-loop control - the intention of this paper is to demonstrate the raw capabilities of induction couplers and provide the motion primitives that will serve as the foundation for controllers. An inspector also needs to rotate in the plane parallel to the surface. The simplest way for induction couplers to produce pure rotation is to act similarly to differential drive wheels. Two couplers with axes parallel to the surface spin in opposite directions.

B. Out-of-Plane Movement

It is more complicated for induction couplers to produce forces and torques that control movement out of the plane parallel to the target surface because the forces from a single induction coupler are limited in their direction.

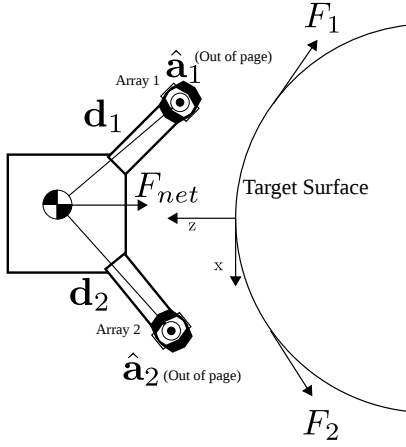


Fig. 4. Configuration for out-of-plane control

The forces generated by spinning arrays are locally almost completely tangential to the surface. For large ω , the ratio of the normal to tangential components of the force increases slightly and can be used to repel away from the surface. However, these forces are small and only act in the $+\hat{z}$ direction, giving no control in $-\hat{z}$. By strategically summing forces across several arrays near different locations on a *non-flat* surface, the inspector can generate larger net forces in both $+\hat{z}$ and $-\hat{z}$.

Rotating two arrays oriented along the \hat{y} with opposing ω will create local forces whose \hat{x} components will cancel and whose \hat{z} components will sum to pull the inspector towards the surface or push it away. This strategy is illustrated in figure 4.

Using locally tangential forces, the inspector can control rotation about the \hat{y} axis by giving each array the same input speed ω . With only two arrays, the torque is coupled with a force - a third array would make the force and torque independent.

IV. SIMULATED DEMONSTRATION

In this section, simulations demonstrate each motion primitive - planar translation, planar rotation, out-of-plane translation, and out-of-plane rotation. In each case, the simulation constrains the inspector to the plane of interest to demonstrate open-loop motion primitives - in practice, a closed loop controller and 2 arrays are absolutely essential to account for motion out of the plane. The model inspector is the size of a small satellite using two motors each with two magnets as induction couplers. The maximum and minimum motor speed inputs match those used in the experimental demonstrations (section V.)

A. Planar Movement

To demonstrate planar movement, the target is a flat plate in the x - y plane, just like figure 3. In figure 5 the inspector drives itself forward and backwards with 30 mN of force by spinning both arrays forward. Note that $\hat{a}_1 = -\hat{a}_2$. In figure 6 the inspector rotates itself with 15 mN-m of torque by counter-spinning each array.

TABLE I
SIMULATION PARAMETERS

Description	value	units
Power Consumed at Maximum Input, P	4	W
Mass m	10.2	kg
Inertia \mathbf{J}	$1.02\mathbf{I}$	kgm^2
Gap in Planar Movement g	1	cm
Conductivity, σ	2.5×10^7	Sm^{-1}
Curvature of non-flat target, κ	0.14	m^{-1}

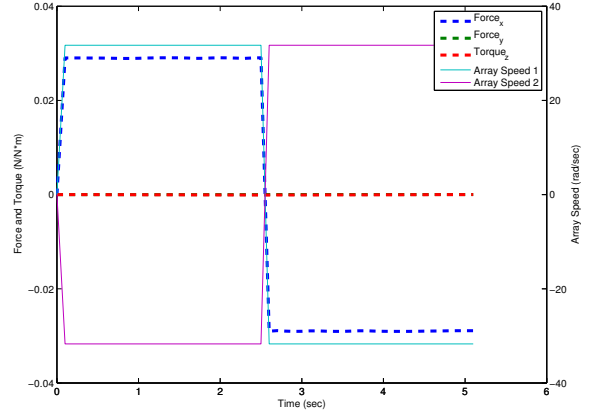


Fig. 5. Simulation of planar translation and reversal

B. Out-of-Plane Movement

To demonstrate planar movement the target is a curved in the x - z plane, just like figure 4. The simulation of \hat{z} motion used a target surface with the same curvature as an ISS module. It demonstrates the ability of an induction-coupled inspector to pull itself towards the surface and then push itself away again before colliding.

V. EXPERIMENTAL DEMONSTRATION

This section presents an experimental demonstration of each motion primitive - planar translation, planar rotation, out-of-plane translation, and out-of-plane rotation in an ideal situation. We constructed two prototype inspection vehicles, each with two spinning magnet arrays - one to demonstrate planar movement, one-to-demonstrate out of plane movement. These inspection vehicles operated on a low-friction air-bearing test bed which allowed them to simulate a space environment with 3 degrees of freedom.

Hardware: The induction couplers were DC hobby gear motors, each with laser-cut cylinder containing a north and south facing 1/2 inch neodymium magnet. A 12V lead-acid battery provided power to the motors, whose power consumption and maximum speed are in table I. An Arduino microprocessor and Xbee radio enabled remote open-loop commands and handled low-level motor control and a visual tag-based tracking system recorded the vehicle's pose.

Considerations: The arrays could not be placed symmetrically about the center of mass due to the constraints of the

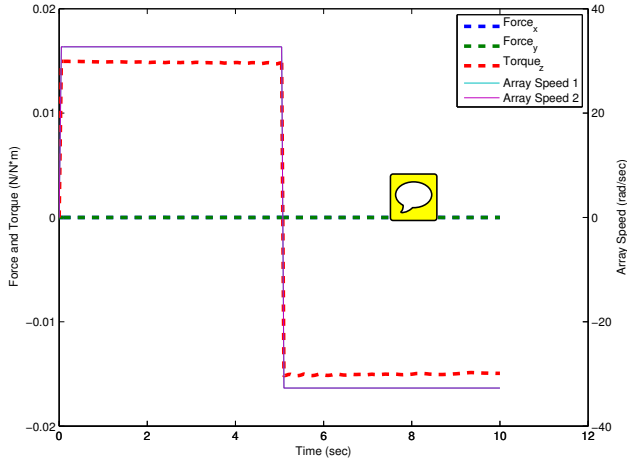


Fig. 6. Simulation of planar rotation and reversal. Note: the control speed is the same for both arrays.

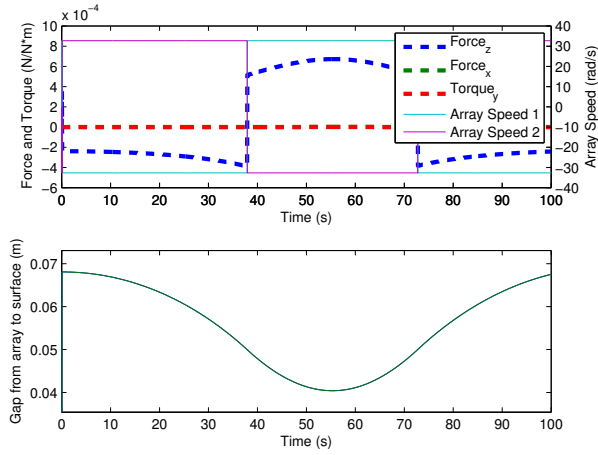


Fig. 7. Simulation of out-of-plane translation - first pulling on, and then pushing away from the target surface

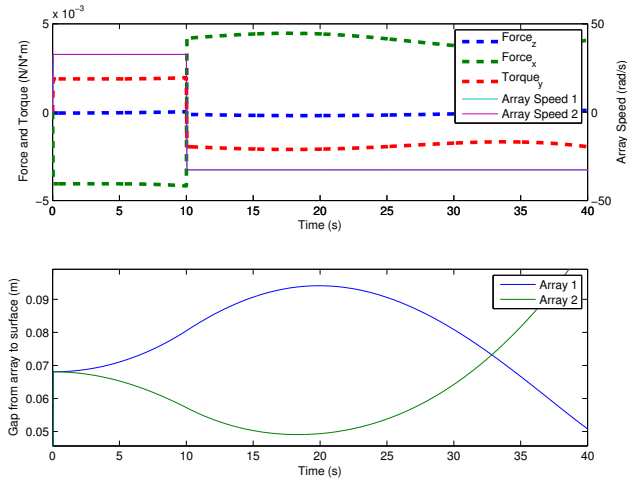


Fig. 8. Simulation of out-of-plane rotation - rotating in the +Y and then -Y direction

test platform. Similarly, the tracking points could not be located at the center of mass because the target occulted it from the tracking system, because the target plate was mounted directly above the vehicle out of necessity. These constraints mean that the experiments serve as a demonstration of the motion, rather than a full model validation.

A. Planar Movement

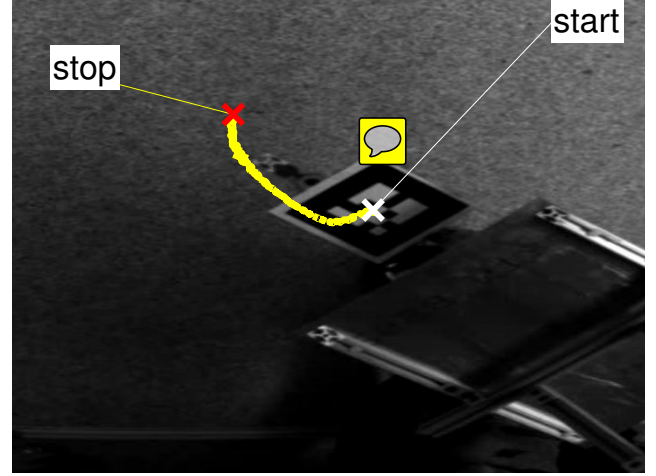


Fig. 9. Trajectory during open-loop orientation and planar translation

Figure 9 shows the trajectory of the inspector during planar translation. The inspector spins both arrays forward to translate forward. The majority of the inspector is obscured because the arrays needed to remain directly under the target surface.

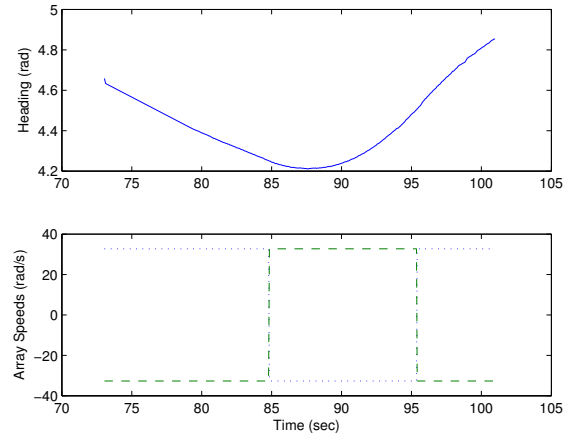


Fig. 10. Heading and control input during open-loop planar rotation

Figure 10 shows a maneuver in which the inspector used induction couplers to rotate itself around the $-z$ axis and then reversed its motion by generating torque around $+z$. Note that $\hat{\mathbf{a}}_1 = \hat{\mathbf{a}}_2$, the opposite of the simulations.

B. Out-of-Plane Movement

The plate used to demonstrate out-of-plane movement has a curvature designed to match the harmony module of the

ISS. The inspector has two arrays, both with axes pointing in the $-y$ direction, out of the page.

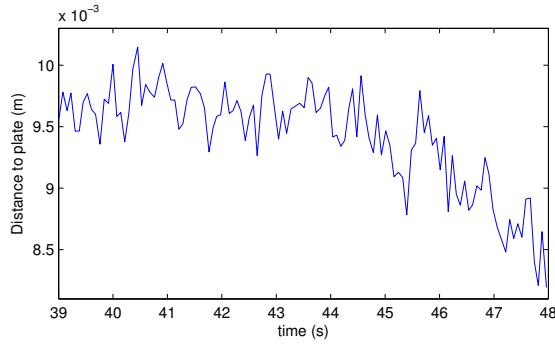
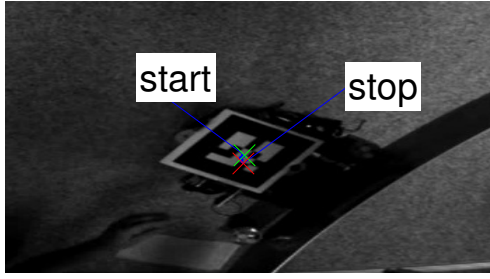


Fig. 11. Top: Overhead view of out-of-plane demonstration Bottom: distance to plate during out-of-plane translation

Figure 11 shows the results from the inspector pulling itself towards the surface. The distance it could travel before colliding with the plate was tiny - a clear reason for closed-loop control. The bottom half of the figure shows the inspector accelerating towards the surface - the distance between the CoM and the plate decreases with an increasing rate.

Figure 12 shows the heading of the inspector as it rotates itself out of the plane about the \hat{y} axis.

VI. CONCLUSION

A robotic on-orbit service vehicle can use induction couplers can produce locomotive forces in all six rigid body degrees of freedom near a conductive surface. Rotating permanent-magnet arrays generate forces perpendicular to both their axes of rotation and the conductive surface. Current-oscillating electromagnets generate forces directly away from the surface. A pair of rotating arrays can produce \hat{x} and \hat{y} forces in the plane of the traversal surface. These two arrays can also produce torques in the \hat{z} direction. This pair of arrays can take advantage of the surface geometry to generate forces in the \hat{z} direction by generating shear forces along a non-flat surface whose \hat{x} and \hat{y} components cancel but whose \hat{z} components add. A single electromagnet generates force in the $+\hat{z}$ direction. The force from the electromagnet can also generate torques based on its relative location to the system's center of mass. These maneuvers are

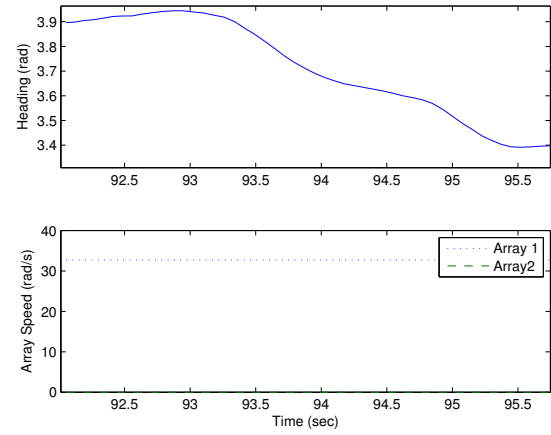


Fig. 12. Heading during out-of-plane rotation

demonstrated in simulations and verified on a low-friction testbed. Future work will focus on two areas - adaptive controllers and movement planning. A robotic inspector will need adaptive controllers to account for induction coupler's strong dependence on poorly known parameters of the environment. The inspector will also need to plan movements carefully because its ability to exert control with an induction coupler is based on both its state and the local geometry.

ACKNOWLEDGMENT

This work was supported by a NSTRF Grant.

REFERENCES

- [1] Jonathan Bird and TA Lipo. Calculating the forces created by an electrodynamic wheel using a 2-D steady-state finite-element method. *Magnetics, IEEE Transactions on*, 44(3):365–372, 2008.
- [2] E Coleshill, L Oshinowo, R Rembala, B Bina, D Rey, and S Sindelar. Dextre: Improving maintenance operations on the International Space Station. *Acta Astronautica*, 64(9-10):869–874, 2009.
- [3] A Ellery. An engineering approach to the dynamic control of space robotic on-orbit servicers. *Proceedings of the Institution of Mechanical Engineers, Part G: Journal of Aerospace Engineering*, 218(2):79–98, 2004.
- [4] A Ellery, J Kreisel, and B Sommer. Ellery, A, J Kreisel, and B Sommer. 2008. The Case for Robotic on-Orbit Servicing of Spacecraft: Spacecraft Reliability Is a Myth. *Acta Astronautica* 63 (5-6): 632648. doi:10.1016/j.actaastro.2008.01.042. ;Go to ISI://WOS/000258632900010.The case for r. *Acta Astronautica*, 63(5-6):632–648, 2008.
- [5] S. Ali a. Moosavian and Evangelos Papadopoulos. Free-flying robots in space: an overview of dynamics modeling, planning and control. *Robotica*, 25(05):537–547, March 2007.
- [6] Takahisa Ohji, Takashi Shinkai, Kenji Amei, and Masaaki Sakui. Application of Lorentz force to a magnetic levitation system for a non-magnetic thin plate. *Journal of Materials Processing Technology*, 181(1-3):40–43, January 2007.
- [7] Nirmal Paudel and Jonathan Z. Bird. Modeling the Dynamic Electromechanical Suspension Behavior of an Electrodynamic Eddy Current Maglev Device. *Progress In Electromagnetics Research B*, 49(February):1–30, 2013.
- [8] Nirmal Paudel and JZ Bird. General 2-D Steady-State Force and Power Equations for a Traveling Time-Varying Magnetic Source Above a Conductive Plate. *Magnetics, IEEE Transactions on*, 48(1):95–100, 2012.
- [9] P C Rem and P A Leest. A model for eddy current separation. 16(96), 1997.

- [10] J H Saleh, E Lamassoure, and D E Hastings. Space systems flexibility provided by on-orbit servicing: Part 1. *Journal of Spacecraft and Rockets*, 39(4):551–560, 2002.
- [11] W.R Smyth. *Static & Dynamic Electricity*. 5th editio edition, 1989.